# A Regulated 48V-to-1V/100A 90.9%-Efficient Hybrid Converter for POL Applications in Data Centers and Telecommunication Systems

Ratul Das and Hanh-Phuc Le
Department of Electrical, Computer and Energy Engineering
University of Colorado, Boulder, Colorado
{ratul.das, hanhphuc}@colorado.edu

Abstract—This paper describes the topology, fundamental operations, and key characteristics of a Dual-Phase Multi-Inductor Hybrid (DP-MIH) Converter for Point of Load (POL) telecommunication and data center applications. The circuit topology employs a unique configuration of switched inductor and capacitor pairs to achieve complete soft charging and native voltage balancing of flying capacitors regardless of mismatches and variations in capacitor and inductor values. The converter topology and its operation are verified by a five-level DP-MIH converter prototype capable of delivering maximum load of 100A at 1V-5V regulated output voltages from a 48V input supply. It achieves 90.9% peak efficiency and 440 w/in³ power density for 48V-to-1V conversion and 95.3% and 2200W/in³ for a 48V-to-5V conversion.

*Index Terms*—Hybrid converter, complete soft-charging, switched capacitor network.

## I. INTRODUCTION

Monthly global mobile data traffic is expected to surpass 100 ExaBytes (EB) in 2023 from around 20 EB today, and merely ~2 EB in 2013[1]. This exponential growth has put a critical pressure on the telecommunication infrastructure, particularly on the architecture of power supply and distribution for this massive need. The most challenging components in the power distribution for telecom power delivery include the point-of-load (POL) converters connected to the 48V intermediate bus as shown in Fig. 1[2]. In designing 48-V PoL converters, transformer-based topologies have been a popular choice with ones that have achieved a good range of efficiencies around ~90%[3] and up to 93.4% [4]. However, to maintain this efficiency range these converters either use a complicated control scheme or have a limited conversion ratio range[5]. In addition, bulky transformers are not desirable for converters that require both high power density and large conversion ratios in applications where isolation is not necessary.

Considering stringent space and load constraints, non-isolated hybrid DC-DC converter topologies have shown promising results. Notable examples include the 48V-to-1V converter reported in [6] aiming at high efficiency and high power density and the 120V-to-0.9V converter in [7] demonstrating extremely large direct conversion ratios. Employing a dual-inductor hybrid (DIH) converter architecture, both converters demonstrated high efficiencies in a moderate load

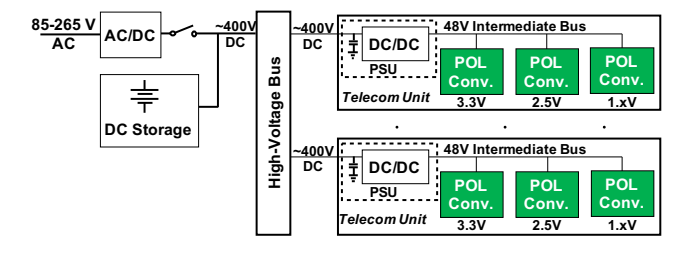


Fig. 1. Telecom power distribution system with 48V POL converters

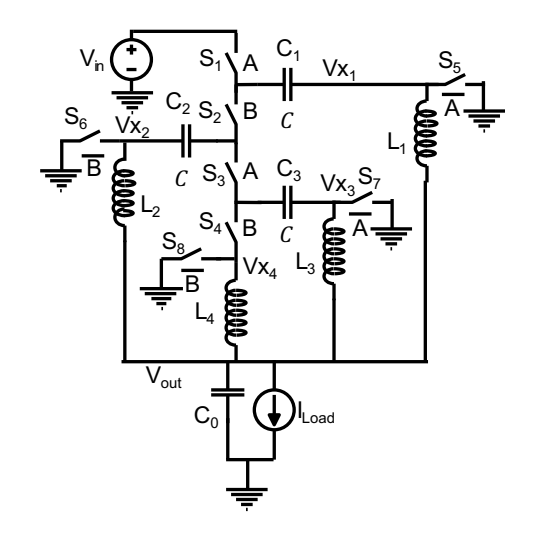


Fig. 2. Dual-Phase Multi-Inductor Hybrid (DP-MIH) Converter

range up to 20A. However, the need for a precise capacitor sizing strategy in [7] or a split phase operation in [6] creates undesirable design complexities that would in turn limit performance at heavier loads. Related works preceding these implementations include the Flying Capacitor Multi Level (FCML) converter reported in [8], the Hybrid Dickson converter in [9], [10], and the multiphase series capacitor Buck converter in [11], [12]. These interesting approaches for non-isolated POL converters still have various short-comings. Particularly, the FCML converter needs a capacitor voltage balancing circuit, the Hybrid Dickson converter requires a split-phase control and published implementations of the series capacitor Buck converter exhibits efficiency limited to ~90%

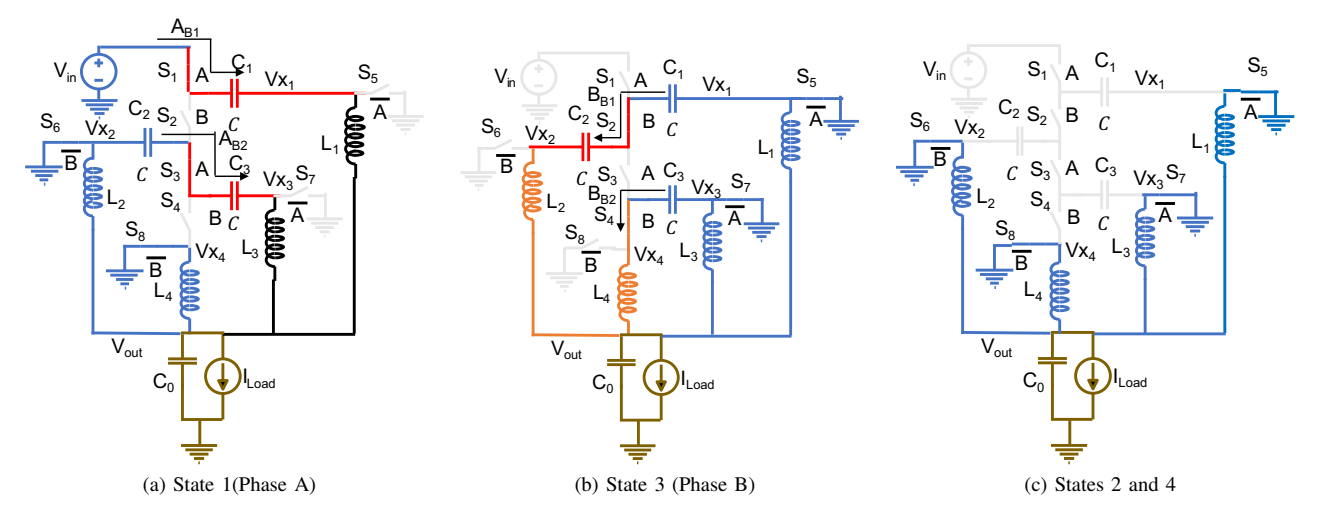


Fig. 3. Operating states of the DP-MIH converter

for a conventional 12V-to-1V conversion. The need for higher efficiency is perhaps self-evident, but larger conversion ratio, low output voltage, and extremely high output current are also critical since they are directly related to the space overhead, thermal managementand hence cost of the input bus distribution, and to enabling technology scaling of the load process.

In order to explore the boundaries of hybrid converter capabilities, in this paper we introduce, analyze and demonstrate a Dual-Phase Multi-Inductor Hybrid (DP-MIH) converter), shown in Fig. 2. The DP-MIH converter is derived as a continuation of work from the Dual Inductor Hybrid (DIH) converters [7], [6], and leverages similarities to the series capacitor Buck converter. Section II describes the converter operation and key characteristics, including complete softcharging operations of all flying capacitors without any specific capacitor sizing or split phase control, inherent capability of providing less voltage stress across switches and inductors, and the benefits of natively balanced inductor currents. Section IV presents experimental results that validate advantageous characteristics in enabling a DP-MIH converter converter prototype to support large conversation ratios from a 48V input to 1V-5V output at a maximum current of 100 A, and a maximum load of 500W. Section V concludes the paper.

### II. OPERATION OF THE DP-MIH CONVERTER

The paper focuses on a four-level version of the DP-MIH converter, ignoring the zero level. It is called a 4-to-1 DP-MIH converter where four is the number of voltage divisions created by the switched capacitor network. The converter circuit is shown in Fig. 2. The converter employs three flying capacitors, four output inductors, and eight switches. As shown in Figs. 3 and 4, the converter is operated with 4 switching states within a switching cycle  $T_S$  where States 1 and 3 are also named energizing phases A and B, respectively. In Fig. 3, red color represents the capacitors getting charged while blue implies discharging. The charged inductors in Fig. 3 have the correspondingly matching color in the inductor

current waveforms of Fig. 4. The first three inductors and flying capacitors form three inductor-capacitor pairs where each capacitor  $C_i$  is directly connected to and soft-charged by inductor  $L_i$  in a charging phase, A or B. The last inductor  $L_4$  only handles soft discharging for the capacitor  $C_3$ . The capacitors are open-circuited and inactive during States 2 and 4. Every inductor is charged in one energizing phase, A or B, and discharges to the output during the other energizing phase and in States 2 and 4. The converter operation converges to a steady state as each capacitor gets equivalent charge and discharge once in every cycle, leading to native capacitor voltage balance and inductor current balance. Charge for each capacitor comes from either input voltage source for  $C_1$  or from a capacitor at an immediate higher level in case of

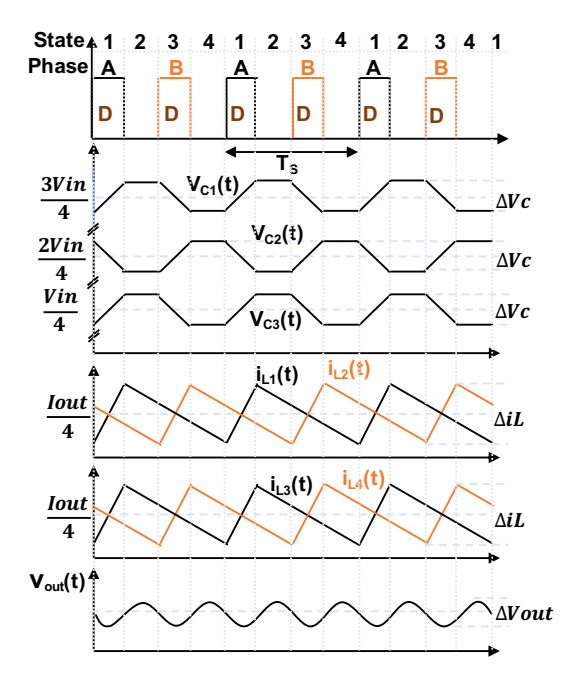


Fig. 4. Operational waveforms of the DP-MIH converter

TABLE I
SWITCHING NODE VOLTAGES IN ENERGIZING STATES

Switching node voltages	State 1 (Phase A)		Switching node voltages	State 3 (Phase B)	
	Start	End	Switching hode voltages	Start	End
$Vx_1(A_{B1})$	$\frac{V_{in}}{4} + \frac{\triangle V_C}{2}$	$\frac{V_{in}}{6} - \frac{\Delta V_C}{2}$	$Vx_2(B_{B1})$	$\frac{V_{in}}{4} + \triangle V_C$	$\frac{V_{in}}{6} - \triangle V_C$
$Vx_3(A_{B2})$	$\frac{V_{in}}{4} + \triangle V_C$	$\frac{V_{in}}{6} - \triangle V_C$	$Vx_4(B_{B2})$	$\frac{V_{in}}{4} + \frac{\Delta V_C}{2}$	$\frac{V_{in}}{6} - \frac{\Delta V_C}{2}$

 $C_2$  and  $C_3$ . In other words, flying capacitors discharge to their immediate lower-level capacitors and inductors except for  $C_3$ , which discharges directly to  $L_4$ . Assuming small voltage ripples in the capacitors and inductor volt-second balance, the steady-state voltages for  $C_1$ ,  $C_2$ , and  $C_3$  are found as  $\frac{3V_{in}}{4}$ ,  $\frac{2V_{in}}{4}$ , and  $\frac{V_{in}}{4}$ , respectively.As the result, the four inductors  $L_{1-4}$  are switched by the same voltage swing of  $\frac{V_{in}}{4}$  at switching nodes  $V_{X1-X4}$ . Each inductor has a charging duty cycle D, i.e. in Phase A or B, making the output voltage  $V_{out} = \frac{DV_{in}}{4}$ . This intuitive conversion ratio result implies a straightforward duty cycle control, allowing for a simple and efficient output voltages at the output and across the flying capacitors for an N-to-1 DP-MIH converter are given as:

$$V_{out} = \frac{DV_{in}}{N} \text{ and } V_{C_k} = \frac{(N-k)V_{in}}{N}$$

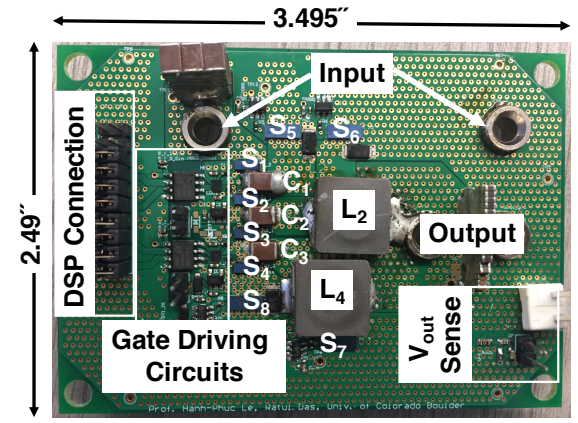
$$where, k = 1, 2, \dots, N-1$$
(1)

For the intended operation of the converter, while Phases A and B need to stay non-overlapped, they are not required to be evenly distributed in the switching cycle. In general, a uniform distribution of interleaving phases is preferred since it minimizes the output current and voltage ripples and enables load transient improvements as similarly found in multi-phase Buck converters.

# III. NATIVE SOFT-CHARGING AND ANALYSIS OF SWITCHING NODE VOLTAGES

Native Soft-charging Feature

The key reason why this DP-MIH converter converter can achieve complete soft charging for all flying capacitors is evident in its operation in which every capacitor is charged or discharged by an inductor in series. No capacitor is shorted



Remaining circuit components are at the bottom side

Fig. 5. A five-level 100-W DP-MIH converter prototype

in parallel with another capacitor or a low impedance source, and thus no capacitor hard charging. This beneficial soft charging is achieved natively without any complicated split-phase control [13], [6] or capacitor sizing strategy [7]. Native soft charging is also achieved regardless of variations and mismatches in flying capacitor values that are oftentimes unavoidable because of different bias voltages and manufacturing tolerance.

Analysis of Switching Node Voltages

As described in the operation of the DP-MIH converter in Section II, all inductors experience an average voltage swing of  $\frac{V_{in}}{4}$  and carries an equal average current of  $\frac{I_{out}}{4}$ . When charging and discharging the flying capacitors, this inductor current generates a voltage ripple of  $\triangle V_C$  across each flying capacitor. In other words, the voltage across each flying capacitor has the same swing of  $\frac{\triangle V_C}{2}$  in addition to its steadystate average voltage. However, in the operation of converter shown in Fig. 3, the charging branches, A<sub>B1</sub>, A<sub>B2</sub>, B<sub>B1</sub>, and B<sub>B2</sub> in the two phases A and B have different number of capacitors, i.e. one or two capacitors. Therefore, the voltage swings at the switching nodes V<sub>X1-X4</sub> have different values, as detailed in Table I. Specifically, during the charging phase  $V_{\rm X2}$  and  $V_{\rm X3}$ experience twice the voltage ripple of V<sub>X1</sub> and V<sub>X4</sub>, leading to larger variations in the current slope L2 and L3 compared with L<sub>1</sub> and L<sub>4</sub> during energizing phase. However, note that if this  $\triangle V_C$  is small compared with  $\frac{V_{in}}{4}$ , the difference in the inductor currents is insignificant. In addition, regardless of this small inductor current mismatch 1) each inductor still maintain a steady periodic waveforms every cycle, and 2) the feature of native soft-charging for all the flying capacitor described above is preserved.

# IV. EXPERIMENTAL RESULTS

In order to validate the converter operations and advantageous characteristics, a DP-MIH converter prototype depicted

TABLE II
MAJOR COMPONENTS

Components	Part information
$S_{1,2,3,4}$	2xEPC2015c
$S_{5,6,7,8}$	2xEPC2023
$C_1$	5.8uF 100V TDK
$C_2$	5uF 100V TDK
$C_3$	4.3uF 100V TDK
$L_{1-4}$	1uH Vishay
Isolators	Si8423
Gate Drivers	LM5114, LMG1205

### TABLE III COMPARISON CHART

Characteristics	DIHC	Series Capacitor	DP-MIH converter
	[6]	Buck[11]	(This work)
Input voltage	40-54 V	12 V	48 V
Output voltage	1-2 V	0.6-1 V	1-5 V
Maximum load current	10 A	60 A	100 A
Maximum power	20 W	60 W	500 W
Number of levels	7	5	5
Capacitor sizing and split	Required	Not required	Not required
phase control			
Peak efficiency	93% @ 1V/4A	90.3% @ 1V/15A	90.9% @ 1V/30A

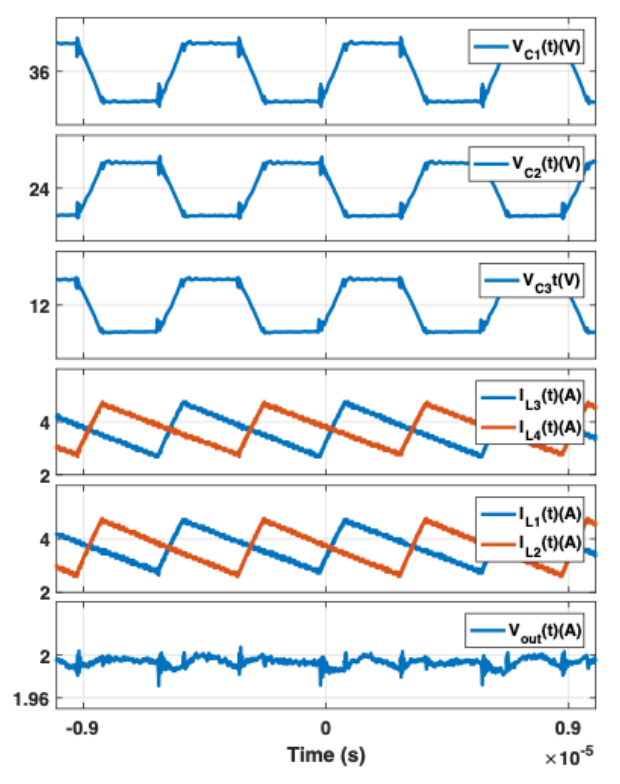


Fig. 6. Measured waveforms of the DP-MIH converter in a 48V-to-2V/15A conversion

in Fig. 5 was implemented. The key components used in the design are listed in Table II. Steady-state waveforms of the four inductor currents, three flying capacitor voltages, and the output voltage are shown in Fig. 6, verifying the converter operation as described in Section II. In these experimental waveforms, the converter was operated at 167-kHz switching frequency, converting a 48V input to a 2V output and 15A load. This switching frequency was specifically chosen to create large ripples on the flying capacitor voltages and inductor currents for convenient measurements. The flying capacitor voltage waveforms in Figure 6 prove that soft charging is achieved for all flying capacitors while the inductor current waveforms demonstrates uniform current distribution for all inductors. To obtain the efficiency in in Fig. 7, the converter was operated at an optimal switching frequency of 333 kHz

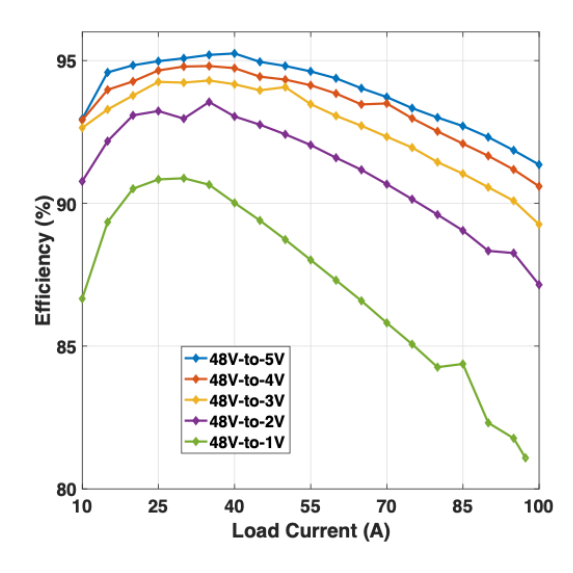


Fig. 7. Measured efficiency of the DP-MIH converter operated at 333 kHz.

for voltage conversions from a 48V input supply to an output regulated at 1V to 5V with a load current up to 100 A. The converter achieves peak efficiencies of 90.9% for a 1V/30A output, 93.6% for 2V/35A and 95.3% for 5V/40A. The efficiency measurements take into account all the powertrain components as well as gate driving losses. Considering key power conversion components, the converter achieves a power density of 440 W/in³ at 1V and 2200 W/in³ at 5V and a current density of 440 A/in³.

The DP-MIH converter converter prototype is compared against previous works in Table III. Compared with the series capacitor Buck converter [11], this DP-MIH converter converter achieves a similar peak efficiencity for 1-V output while supporting 4X conversion ratios, i.e. from 48V input instead of 12V, 1.6X maximum current capability, and 2X current at peak efficiency. Compared with the DIH converter in [6],it achieves 10X maximum output current and 25X output power.

# V. CONCLUSION

In this paper, a Dual-Phase Multi-Inductor Hybrid (DP-MIH) converter was presented with operation analysis and

experimental results. The converter exhibits a superior configuration and performance at higher loads compared with the state-of-the-art designs because of its unique hybrid topology configuration and operation that enables complete native soft charging in all flying capacitors without requiring any complex control or capacitor sizing method. A 500-W experimental prototype successfully demonstrates the intended operation and characteristics, achieving 90.9% peak efficiency for a 48V-to-1V conversion and regulating an output up to 5 V with loads up to 100A.

### ACKNOWLEDGMENT

This research work received financial and technical supports from NSF ECCS program award No. 1810470, Oracle, Power America, Lockheed Martin and the University of Colorado Boulder.

### REFERENCES

- R. Moller, "Ericsson Mobility Report November 2017," Ericsson, Tech. Rep.
- [2] M. Salato, "Re-architecting 48v power systems with a novel non-isolated bus converter," in 2015 IEEE International Telecommunications Energy Conference (INTELEC), Osaka, Japan, Oct. 2015, pp. 1–4.
- [3] A. Kumar, S. Pervaiz, and K. K. Afridi, "Single-stage isolated 48v-to-1.8v point-of-load converter utilizing an impedance control network and integrated magnetic structures," in 2017 IEEE 18th Workshop on Control and Modeling for Power Electronics (COMPEL), Stanford, CA, Jul. 2017, pp. 1–7.
- [4] M. Ahmed, C. Fei, F. C. Lee, and Q. Li, "High-efficiency high-power-density 48/1v sigma converter voltage regulator module," in 2017 IEEE Applied Power Electronics Conference and Exposition (APEC), Tampa, FL, Mar. 2017, pp. 2207–2212.
- [5] M. H. Ahmed, C. Fei, V. Li, F. C. Lee, and Q. Li, "Startup and control of high efficiency 48/1v sigma converter," in 2017 IEEE Energy Conversion Congress and Exposition (ECCE), Cincinnati, OH, Oct. 2017, pp. 2010– 2016

- [6] G. S. Seo, R. Das, and H. P. Le, "A 95%-Efficient 48v-to-1v/10a VRM Hybrid Converter Using Interleaved Dual Inductors," in 2018 IEEE Energy Conversion Congress and Exposition (ECCE), Portland, Oregon, Sep. 2018.
- [7] R. Das, G. S. Seo, and H. P. Le, "A 120v-to-1.8v 91.5%-Efficient 36-W Dual-Inductor Hybrid Converter with Natural Soft-charging Operations for Direct Extreme Conversion Ratios," in 2018 IEEE Energy Conversion Congress and Exposition (ECCE), Portland, Oregon, Sep. 2018.
- [8] J. S. Rentmeister and J. T. Stauth, "A 48v:2v flying capacitor multilevel converter using current-limit control for flying capacitor balance," in 2017 IEEE Applied Power Electronics Conference and Exposition (APEC), Tamp, FL, Mar. 2017, pp. 367–372.
- [9] Y. Lei, Z. Ye, and R. C. N. Pilawa-Podgurski, "A GaN-based 97% efficient hybrid switched-capacitor converter with lossless regulation capability," in 2015 IEEE Energy Conversion Congress and Exposition (ECCE), Montreal, QC, Sep. 2015, pp. 4264–4270.
- [10] Y. Lei, R. May, and R. Pilawa-Podgurski, "Split-Phase Control: Achieving Complete Soft-Charging Operation of a Dickson Switched-Capacitor Converter," *IEEE Transactions on Power Electronics*, vol. 31, no. 1, pp. 770–782, Jan. 2016.
- [11] K. Matsumoto, K. Nishijima, T. Sato, and T. Nabeshima, "A two-phase high step down coupled-inductor converter for next generation low voltage CPU," in 8th International Conference on Power Electronics ECCE Asia, May 2011, pp. 2813–2818.
- [12] P. S. Shenoy, M. Amaro, J. Morroni, and D. Freeman, "Comparison of a Buck Converter and a Series Capacitor Buck Converter for High-Frequency, High-Conversion-Ratio Voltage Regulators," *IEEE Transactions on Power Electronics*, vol. 31, no. 10, pp. 7006–7015, Oct. 2016.
- [13] Y. Lei, R. May, and R. Pilawa-Podgurski, "Split-Phase Control: Achieving Complete Soft-Charging Operation of a Dickson Switched-Capacitor Converter," *IEEE Transactions on Power Electronics*, vol. 31, no. 1, pp. 770–782, Jan. 2016. [Online]. Available: http://ieeexplore.ieee.org/document/7041205/